Hindawi Publishing Corporation
Journal of Control Science and Engineering
Volume 2016, Article ID 4195491, 14 pages
http://dx.doi.org/10.1155/2016/4195491

*Research Article*

# Stability Analysis of a Helicopter with an External Slung Load System

**Kary Thanapalan**

*Faculty of Computing, Engineering and Science, University of South Wales, Pontypridd CF37 1DL, UK*

Correspondence should be addressed to Kary Thanapalan; kary.thanapalan@southwales.ac.uk

Received 20 November 2015; Revised 18 April 2016; Accepted 4 May 2016

Academic Editor: Francisco Gordillo



This paper describes the stability analysis of a helicopter with an underslung external load system. The Lyapunov second method is considered for the stability analysis. The system is considered as a cascade connection of uncertain nonlinear system. The stability analysis is conducted to ensure the stabilisation of the helicopter system and the positioning of the underslung load at hover condition. Stability analysis and numerical results proved that if desired condition for the stability is met, then it is possible to locate the load at the specified position or its neighbourhood.

## 1. Introduction

Recently, research on helicopter carrying external underslung loads has gained great attention in the aerospace research community for the past few decades due to the reevaluation and extension of the ADS-33 and the inherent stability problems associated with this system [1–3]. Helicopters have the ability to carry large and bulky loads externally on a sling. This capability is important in many applications, ranging from lifting heavy loads to saving life. Importantly, when lives are under risk and rapid rescue operations are needed, this operation is vital. The stability of the helicopter will be disturbed by the underslung load, which is a huge obstacle for an accurate pickup or placement of the loads [4]. Thus, it is necessary to resolve the stability problems associated with the system to ensure the stabilisation of the helicopter system and the positioning of the underslung load under various complicated situations.

From the review of popular helicopter control methods, it is clear that, in the past years, considerable attention has been paid to the design of controller to obtain a satisfactory helicopter handling quality [5]. The control problem has been tackled using different approaches ranging from linear quadratic control [6], eigenstructure assignment [7], classical SISO techniques [8], to sliding mode control [9]. Apart from the methods emphasised above there are many other techniques which are reported for complex modern control system design ranging from quantitative feedback theory to singular perturbation method [10].

The extensive studies of the reported controller design methods evidenced that the helicopter control and the control of a helicopter with an external underslung load are very active research areas. The research in this area is mainly motivated by the factor that the current control methods cannot provide full satisfaction to the desired design requirements on flight handling quality, stability, robustness, and so forth.

In this paper, stability analysis for the helicopter with an underslung external load system is discussed. The key advantage of the proposed method is that the analysis takes the system uncertainty into account. The proposed method can give a guaranteed stability region for the systems considered. The paper begins by presenting a mathematical model of the system and then describing the stability analysis with a numerical example to illustrate the applicability, accuracy, and effectiveness of the proposed method.

## 2. System Model

Considering the control of a helicopter with an underslung load, the dynamical models of both the helicopter and load have some terms which are uncertain. The uncertainties may arise from the helicopter to carry an unknown load or the immeasurable parameters in the dynamical models. The uncertainties may also arise from computational errors of the dynamical effects such as aerodynamics. Therefore for a realistic model uncertainties must be taken into account during the controller design.

A mathematical model of the helicopter described in [11] and an underslung load model presented in [4] are adopted in this work. Considering the two models, a mathematical model for a helicopter carrying an underslung load can be obtained.

Firstly, the underslung load is considered to be suspended from a single suspension point that is subject to motion and therefore modelled as a driven spherical pendulum. The equations that describe the load dynamics are obtained by first considering motion with reference to the longitudinal suspension angle $\theta_L$ in the $X$-$Z$ plane (Figure 1). This is then repeated for the lateral case involving $\varphi_L$ and the $Y$-$Z$ plane. These are then combined to obtain the model for the motion of the load. The underslung load system has six inputs, longitudinal, lateral, and vertical velocities together with the corresponding accelerations of the helicopter, whilst the outputs are the longitudinal and lateral directional suspension angles. The load is subject to an isotropic aerodynamic force (proportional to the square of its airspeed) such as what would be experienced by a spherical shaped load. Aerodynamic interaction with the helicopter that may occur, for example, due to rotor downwash, has been ignored. Finally, the sling itself is assumed to be rigid and contribute zero aerodynamic force of its own. With these assumptions, the equations governing the load motion can be derived as follows.

For the case of the longitudinal motion in the $X$-$Z$ plane, the mathematical model is described below:

$$\begin{aligned}
\ddot{\theta}_L = & -\frac{g}{l_x}\sin\theta_L + \frac{\cos\theta_L}{l_x}\ddot{X}_0 + \frac{\sin\theta_L}{l_x}\ddot{Z}_0 \\
& + \frac{k_D \operatorname{sign}(\dot{X}_L)\cos\theta_L}{M_L l_x}\dot{X}_0^2 + \frac{k_D \operatorname{sign}(\dot{Z}_L)\sin\theta_L}{M_L l_x}\dot{Z}_0^2 \\
& - \frac{2k_D}{M_L}\left(\operatorname{sign}(\dot{X}_L)\cos^2\theta_L \dot{X}_0\right. \\
& \left. + \operatorname{sign}(\dot{Z}_L)\sin^2\theta_L \dot{Z}_0\right)\dot{\theta}_L - k_\theta \dot{\theta}_L \\
& + \frac{k_D l_x}{M_L}\left[\operatorname{sign}(\dot{X}_L)\cos^3\theta_L + \operatorname{sign}(\dot{Z}_L)\sin^3\theta_L\right]\dot{\theta}_L^2.
\end{aligned} \tag{1}$$

Define $\tilde{\theta}_L = [\theta_L \ \ \dot{\theta}_L]^T = [\theta_{L_1} \ \ \theta_{L_2}]^T$; then the load model can be rewritten as follows:

$$\dot{\theta}_{L_1} = \theta_{L_2}, \tag{2a}$$

$$\begin{aligned}
\dot{\theta}_{L_2} = & \frac{-g}{l_x}\sin\theta_{L_1} + \frac{k_D l_x}{M_L}\left[\operatorname{sign}(\dot{X}_L)\cos^3\theta_{L_1}\right. \\
& \left. + \operatorname{sign}(\dot{Z}_L)\sin^3\theta_{L_1}\right]\theta_{L_2}^2 - k_\theta \theta_{L_2} \\
& + \left(\frac{k_D \operatorname{sign}(\dot{X}_L)\cos\theta_{L_1}}{M_L l_x}\right)\dot{X}_0^2 \\
& + \left(\frac{k_D \operatorname{sign}(\dot{Z}_L)\sin\theta_{L_1}}{M_L l_x}\right)\dot{Z}_0^2 + \frac{\cos\theta_{L_1}}{l_x}\ddot{X}_0 \\
& + \frac{\sin\theta_{L_1}}{l_x}\ddot{Z}_0 - \frac{2k_D}{M_L}\left(\operatorname{sign}(\dot{X}_L)\cos^2\theta_{L_1}\dot{X}_0\right. \\
& \left. + \operatorname{sign}(\dot{Z}_L)\sin^2\theta_{L_1}\dot{Z}_0\right)\theta_{L_2}.
\end{aligned} \tag{2b}$$

The helicopter model is considered as the second subsystem. To simplify the analysis, the linear helicopter model [4] is considered, which is expressed in the state space form $\dot{\overline{x}}_H(t) = A\overline{x}_H(t) + B\overline{u}(t)$:

$$\begin{bmatrix} \dot{\phi} \\ \dot{\theta} \\ \dot{\psi} \\ \dot{u} \\ \dot{v} \\ \dot{w} \\ \dot{p} \\ \dot{q} \\ \dot{r} \end{bmatrix} = \begin{bmatrix} 0 & 0 & 0 & 0 & 0 & 0 & 1 & 0 & 0 \\ 0 & 0 & 0 & 0 & 0 & 0 & 0 & 1 & 0 \\ 0 & 0 & 0 & 0 & 0 & 0 & 0 & 0 & 1 \\ 0 & -g\cos\theta_e & 0 & X_u & X_v & X_w & X_p & (X_q - w_e) & (X_r - v_e) \\ g & 0 & 0 & Y_u & Y_v & Y_w & (Y_p + w_e) & Y_q & (Y_r - u_e) \\ 0 & -g\sin\theta_e & 0 & Z_u & Z_v & Z_w & (Z_p - v_e) & (Z_q + u_e) & Z_r \\ 0 & 0 & 0 & L_u & L_v & L_w & L_p & L_q & L_r \\ 0 & 0 & 0 & M_u & M_v & M_w & M_p & M_q & M_r \\ 0 & 0 & 0 & N_u & N_v & N_w & N_p & N_q & N_r \end{bmatrix} \begin{bmatrix} \phi \\ \theta \\ \psi \\ u \\ v \\ w \\ p \\ q \\ r \end{bmatrix} + \begin{bmatrix} 0 & 0 & 0 & 0 \\ 0 & 0 & 0 & 0 \\ 0 & 0 & 0 & 0 \\ X_{\theta_{1c}} & X_{\theta_{1s}} & X_{\theta_0} & X_{\theta_{0T}} \\ Y_{\theta_{1c}} & Y_{\theta_{1s}} & Y_{\theta_0} & Y_{\theta_{0T}} \\ Z_{\theta_{1c}} & Z_{\theta_{1s}} & Z_{\theta_0} & Z_{\theta_{0T}} \\ L_{\theta_{1c}} & L_{\theta_{1s}} & L_{\theta_0} & L_{\theta_{0T}} \\ M_{\theta_{1c}} & M_{\theta_{1s}} & M_{\theta_0} & M_{\theta_{0T}} \\ N_{\theta_{1c}} & N_{\theta_{1s}} & N_{\theta_0} & N_{\theta_{0T}} \end{bmatrix} \begin{bmatrix} \theta_{1c} \\ \theta_{1s} \\ \theta_0 \\ \theta_{0T} \end{bmatrix}. \tag{3}$$

For linearization, it is assumed that the external forces $X$, $Y$, and $Z$ and moments $L$, $M$, and $N$ can be represented as analytic functions of the disturbed motion variables and their derivatives [4]. Thus the forces and moments can be written

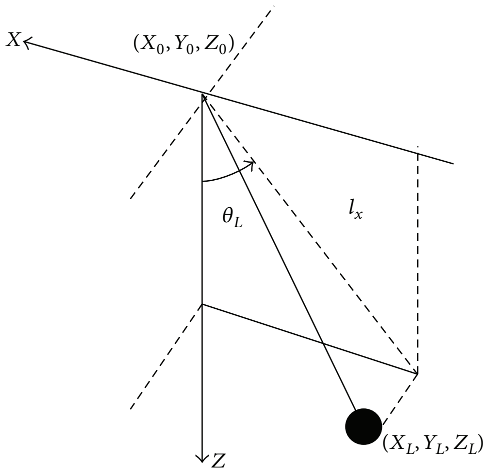


Figure 1: Coordinate system for the longitudinal motion in the $X$-$Z$ plane.

in Taylor's expansion form. Then, the linearized equations of motion about a general trim condition can be written as in the state space form $\dot{\overline{x}} = A\overline{x} + B\overline{u}$ and the system matrix $A$ and control matrix $B$ are derived from the partial derivatives of the nonlinear function $\overline{F}$, that is,

$$\begin{gathered} \dot{\overline{x}} = \overline{F}\left(\overline{x}, \overline{u}, t\right), \\ A = \left(\frac{\partial \overline{F}}{\partial \overline{x}}\right)_{\overline{x}=\overline{x}_e}, \\ B = \left(\frac{\partial \overline{F}}{\partial \overline{u}}\right)_{\overline{x}=\overline{x}_e}. \end{gathered} \tag{4}$$

Now, the longitudinal rotational motion is described by the pitch angle $\theta$ and pitch rate $q$ together with the translation motion components $u, w$ so the equation of longitudinal motion can be written as follows:

$$\begin{bmatrix} \dot{\theta} \\ \dot{q} \\ \dot{u} \\ \dot{w} \end{bmatrix} = \begin{bmatrix} 0 & 1 & 0 & 0 \\ 0 & M_q & M_u & M_w \\ -g\cos\theta_e & \left(X_q - w_e\right) & X_u & X_w \\ -g\sin\theta_e & \left(Z_q - u_e\right) & Z_u & Z_w \end{bmatrix} \begin{bmatrix} \theta \\ q \\ u \\ w \end{bmatrix} + \begin{bmatrix} 0 & 0 \\ M_{\theta_{1s}} & M_{\theta_0} \\ X_{\theta_{1s}} & X_{\theta_0} \\ Z_{\theta_{1s}} & Z_{\theta_0} \end{bmatrix} \begin{bmatrix} \theta_{1s} \\ \theta_0 \end{bmatrix}. \tag{5}$$

By applying a linear transformation $\overline{T}$ such that $x_H(t) = \overline{T}z(t)$ and $\overline{T}$ is defined by

$$\overline{T} = \begin{bmatrix} 1 & 0 & 0 & 0 \\ 0 & 1 & a_{11} & a_{12} \\ 0 & 0 & 1 & 0 \\ 0 & 0 & 0 & 1 \end{bmatrix}, \tag{6}$$

where

$$\begin{gathered} a_{11} = -\frac{Z_{\theta_{1s}}M_{\theta_0} - Z_{\theta_0}M_{\theta_{1s}}}{X_{\theta_{1s}}Z_{\theta_0} - Z_{\theta_{1s}}X_{\theta_0}}, \\ a_{12} = -\frac{X_{\theta_0}M_{\theta_{1s}} - X_{\theta_{1s}}M_{\theta_0}}{X_{\theta_{1s}}Z_{\theta_0} - Z_{\theta_{1s}}X_{\theta_0}}, \end{gathered} \tag{7}$$

and letting $\overline{q} = (q - a_{11}u - a_{12}w)$, then the system equation (5) is transformed into the following form:

$$\begin{bmatrix} \dot{\theta} \\ \dot{\overline{q}} \\ \dot{u} \\ \dot{w} \end{bmatrix} = \begin{bmatrix} X_{11} & X_{12} & X_{13} & X_{14} \\ X_{21} & X_{22} & X_{23} & X_{24} \\ X_{31} & X_{32} & X_{33} & X_{34} \\ X_{41} & X_{42} & X_{43} & X_{44} \end{bmatrix} \begin{bmatrix} \theta \\ \overline{q} \\ u \\ w \end{bmatrix} + \begin{bmatrix} 0 & 0 \\ B_{21} & B_{22} \\ X_{\theta_{1s}} & X_{\theta_0} \\ Z_{\theta_{1s}} & Z_{\theta_0} \end{bmatrix} \begin{bmatrix} \theta_{1s} \\ \theta_0 \end{bmatrix}, \tag{8}$$

where

$$\begin{aligned} X_{11} &= 0, \\ X_{12} &= 1, \\ X_{13} &= a_{11}, \\ X_{14} &= a_{12} \\ X_{21} &= \left(a_{11}g\cos\theta_e + a_{12}g\sin\theta_e\right), \\ X_{22} &= \left(M_q - a_{11}\left(X_q - w_e\right) - a_{12}\left(Z_q - u_e\right)\right) \\ X_{23} &= \left(M_q - a_{11}\left(X_q - w_e\right) - a_{12}\left(Z_q + u_e\right)\right)a_{11} \\ &\quad + \left(M_u - a_{11}X_u - a_{12}Z_u\right) \\ X_{24} &= \left(M_q - a_{11}\left(X_q - w_e\right) - a_{12}\left(Z_q + u_e\right)\right)a_{12} \\ &\quad + \left(M_w - a_{11}X_w - a_{12}Z_w\right), \\ X_{31} &= -g\cos\theta_e, \\ X_{32} &= \left(X_q - w_e\right), \\ X_{33} &= \left(X_q - w_e\right)a_{11} + X_u, \\ X_{34} &= \left(X_q - w_e\right)a_{11} + X_w, \\ X_{41} &= \left(-g\sin\theta_e\right), \\ X_{42} &= \left(Z_q + u_e\right), \\ X_{43} &= \left(Z_q + u_e\right)a_{11} + Z_u, \\ X_{44} &= \left(Z_q + u_e\right)a_{12} + Z_w, \end{aligned}$$

$$B_{21} = \left(M_{\theta_{1s}} - a_{11}X_{\theta_{1s}} - a_{12}Z_{\theta_{1s}}\right),$$
$$B_{22} = \left(M_{\theta_0} - a_{11}X_{\theta_0} - a_{11}Z_{\theta_0}\right). \quad (9)$$

Using (8) the system model can be rearranged to include the variables $\theta$ and $\overline{q}$ into the load model. For the stability analysis purpose, an extra term is introduced into the system model, which is zero with the expression

$$\frac{\kappa_1 k_D \operatorname{sign}(\dot{X}_L)\cos\theta_{L_1} u}{M_L l_x} + \frac{\kappa_2 k_D \operatorname{sign}(\dot{X}_L)\cos\theta_{L_1} w}{M_L l_x} - \frac{\kappa_1 k_D \operatorname{sign}(\dot{X}_L)\cos\theta_{L_1} u}{M_L l_x} - \frac{\kappa_2 k_D \operatorname{sign}(\dot{X}_L)\cos\theta_{L_1} w}{M_L l_x}, \quad (10)$$

where $\kappa_i > 0$ $(i = 1, 2)$ are small positive constants.

With this arrangement for the longitudinal motion of the helicopter with an underslung load combined system model can be written as follows:

$$\dot{\overline{\theta}}_L(t) = f_1(\overline{\theta}_L(t)) + G_1(\overline{\theta}_L(t))\left[p(x_H(t)) + q(\overline{\theta}_L(t), x_H(t))\right] + H(t, \overline{\theta}_L, x_H(t)) \quad (11a)$$

$$\dot{x}_H(t) = f_2(\overline{\theta}_L(t), x_H(t)) + G_2\tilde{u}(t), \quad (11b)$$

where

$$\overline{\theta}_L(t) = [\theta_{L_1}\ \ \theta_{L_2}\ \ \theta\ \ \overline{q}]^T,$$
$$x_H = [u\ \ w]^T,$$
$$\tilde{u}(t) = [\theta_{1s}\ \ \theta_0]^T,$$
$$p(x_H) = [u^2 + \kappa_1 u\ \ w^2 + \kappa_2 w]^T,$$
$$f_1(\overline{\theta}_L(t)) = \begin{bmatrix} \theta_{L_2} \\ \frac{-g}{l_x}\sin\theta_{L_1} + \frac{k_D l_x}{M_L}\left(\operatorname{sign}(\dot{X}_L)\cos^3\theta_{L_1} + \operatorname{sign}(\dot{Z}_L)\sin^3\theta_{L_1}\right)\theta_{L_2}^2 - k_\theta\theta_{L_2} \\ \overline{q} \\ (X_{21}\theta + X_{22}\overline{q}) \end{bmatrix}$$
$$G_1(\overline{\theta}_L(t)) = \begin{bmatrix} 0 & 0 \\ \frac{k_D \operatorname{sign}(\dot{X}_L)\cos\theta_{L_1}}{M_L l_x} & \frac{k_D \operatorname{sign}(\dot{Z}_L)\sin\theta_{L_1}}{M_L l_x} \\ 0 & 0 \\ 0 & 0 \end{bmatrix}$$
$$q(\overline{\theta}_L(t), x_H(t)) = \begin{bmatrix} 0 \\ \frac{\cos\theta_{L_1}}{l_x}\dot{u} + \frac{\sin\theta_{L_1}}{l_x}\dot{w} - \frac{2k_D}{M_L}\left(\operatorname{sign}(\dot{X}_L)\cos^2\theta_{L_1} u + \operatorname{sign}(\dot{Z}_L)\sin^2\theta_{L_1} w\right)\theta_{L_2} - \frac{\kappa_1 k_D \operatorname{sign}(\dot{X}_L)\cos\theta_{L_1} u}{M_L l_x} - \frac{\kappa_2 k_D \operatorname{sign}(\dot{X}_L)\cos\theta_{L_1} w}{M_L l_x} \end{bmatrix}$$
$$H(t, \overline{\theta}_L(t), x_H(t)) = \begin{bmatrix} 0 \\ 0 \\ (a_{11}u + a_{12}w) \\ X_{23}u + X_{24}w \end{bmatrix},$$
$$f_2(\overline{\theta}_L(t), x_H(t)) = \begin{bmatrix} (X_{31}\theta + X_{32}\overline{q} + X_{33}u + X_{34}w) \\ (X_{41}\theta + X_{42}\overline{q} + X_{43}u + X_{44}w) \end{bmatrix},$$
$$G_2 = \begin{bmatrix} X_{\theta_{1s}} & X_{\theta_0} \\ Z_{\theta_{1s}} & Z_{\theta_0} \end{bmatrix}. \quad (12)$$

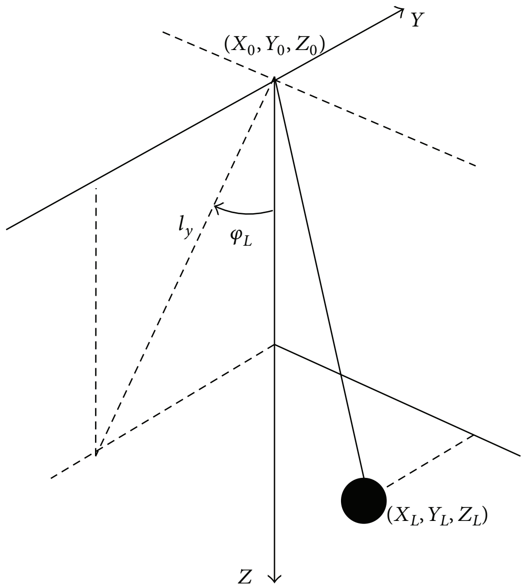


FIGURE 2: Coordinate system for the lateral motion in the $Y$-$Z$ plane.

It is assumed that the longitudinal motion is primarily controlled by longitudinal cyclic commands ($\theta_{1s}$) and main rotor collective $\theta_0$.

For the case of the lateral motion in the $Y$-$Z$ plane, with the coordinate system described in Figure 2, the load model is

$$\begin{aligned}\ddot{\varphi}_{L_{yz}} &= -\frac{g}{l_y}\sin\varphi_{L_{yz}} + \frac{\cos\varphi_{L_{yz}}}{l_y}\ddot{Y}_0 + \frac{\sin\varphi_{L_{yz}}}{l_y}\ddot{Z}_0 \\ &+ \frac{k_D \operatorname{sign}(\dot{Y}_L)\cos\varphi_{L_{yz}}}{M_L l_y}\dot{Y}_0^2 \\ &+ \frac{k_D \operatorname{sign}(\dot{Z}_L)\sin\varphi_{L_{yz}}}{M_L l_y}\dot{Z}_0^2 \\ &- \frac{2k_D}{M_L}\left(\operatorname{sign}(\dot{Y}_L)\cos^2\varphi_{L_{yz}}\dot{Y}_0\right. \\ &\left.+ \operatorname{sign}(\dot{Z}_L)\sin^2\varphi_{L_{yz}}\dot{Z}_0\right)\dot{\varphi}_L - k_\varphi\dot{\varphi}_L \\ &+ \frac{k_D l_y}{M_L}\left[\operatorname{sign}(\dot{Y}_L)\cos^3\varphi_{L_{yz}} + \operatorname{sign}(\dot{Z}_L)\sin^3\varphi_{L_{yz}}\right] \\ &\cdot \dot{\varphi}_{L_{yz}}^2.\end{aligned} \tag{13}$$

Define $\tilde{\varphi}_L = [\varphi_L \;\; \dot{\varphi}_L]^T = [\varphi_{L_1} \;\; \varphi_{L_2}]^T$; then the model can be written as follows:

$$\dot{\varphi}_{L_1} = \varphi_{L_2} \tag{14a}$$

$$\begin{aligned}\dot{\varphi}_{L_2} &= \frac{-g}{l_y}\sin\varphi_{L_1} + \frac{k_D l_y}{M_L}\left[\operatorname{sign}(\dot{Y}_L)\cos^3\varphi_{L_1}\right. \\ &\left.+ \operatorname{sign}(\dot{Z}_L)\sin^3\varphi_{L_1}\right]\varphi_{L_2}^2 - k_\varphi\varphi_{L_2} \\ &+ \left(\frac{k_D \operatorname{sign}(\dot{Y}_L)\cos\varphi_{L_1}}{M_L l_y}\right)\dot{Y}_0^2 \\ &+ \left(\frac{k_D \operatorname{sign}(\dot{Z}_L)\sin\varphi_{L_1}}{M_L l_y}\right)\dot{Z}_0^2 + \frac{\cos\varphi_{L_1}}{l_y}\ddot{Y}_0 \\ &+ \frac{\sin\varphi_{L_1}}{l_y}\ddot{Z}_0 - \frac{2k_D}{M_L}\left(\operatorname{sign}(\dot{Y}_L)\cos^2\varphi_{L_1}\dot{Y}_0\right. \\ &\left.+ \operatorname{sign}(\dot{Z}_L)\sin^2\varphi_{L_1}\dot{Z}_0\right)\varphi_{L_2}.\end{aligned} \tag{14b}$$

Now, for the helicopter model the lateral rotational motion is described by the roll angle $\phi$ and roll rate $p$ together with the translation motion components $v$, $w$ so the equation of lateral motion can be written as follows:

$$\begin{aligned}\begin{bmatrix}\dot{\phi}\\ \dot{p}\\ \dot{v}\\ \dot{w}\end{bmatrix} &= \begin{bmatrix}0 & 1 & 0 & 0\\ 0 & L_p & L_v & L_w\\ g & (Y_p - w_e) & Y_v & Y_w\\ 0 & (Z_p - v_e) & Z_v & Z_w\end{bmatrix}\begin{bmatrix}\phi\\ p\\ v\\ w\end{bmatrix} \\ &+ \begin{bmatrix}0 & 0\\ L_{\theta_{1c}} & L_{\theta_{0T}}\\ Y_{\theta_{1c}} & Y_{\theta_{0T}}\\ Z_{\theta_{1c}} & Z_{\theta_{0T}}\end{bmatrix}\begin{bmatrix}\theta_{1c}\\ \theta_{0T}\end{bmatrix},\end{aligned} \tag{15}$$

now using a linear transformation $\overline{T}_1$ such that $x_H(t) = \overline{T}_1 z(t)$ and $\overline{T}_1$ is defined by

$$\overline{T}_1 = \begin{bmatrix}1 & 0 & 0 & 0\\ 0 & 1 & b_{11} & b_{12}\\ 0 & 0 & 1 & 0\\ 0 & 0 & 0 & 1\end{bmatrix}, \tag{16}$$

where

$$\begin{aligned}b_{11} &= -\frac{Z_{\theta_{1c}}L_{\theta_{0T}} - Z_{\theta_{0T}}L_{\theta_{1c}}}{Y_{\theta_{1c}}Z_{\theta_{0T}} - Z_{\theta_{1c}}Y_{\theta_{0T}}}, \\ b_{12} &= -\frac{Y_{\theta_{0T}}L_{\theta_{1c}} - Y_{\theta_{1c}}L_{\theta_{0T}}}{Y_{\theta_{1c}}Z_{\theta_{0T}} - Z_{\theta_{1c}}Y_{\theta_{0T}}}.\end{aligned} \tag{17}$$

Let $\overline{p} = (p - b_{11}v - b_{12}w)$; then (15) can be written in the following form:

$$\begin{bmatrix} \dot{\phi} \\ \dot{\overline{p}} \\ \dot{v} \\ \dot{w} \end{bmatrix} = \begin{bmatrix} Y_{11} & Y_{12} & Y_{13} & Y_{14} \\ Y_{21} & Y_{22} & Y_{23} & Y_{24} \\ Y_{31} & Y_{32} & Y_{33} & Y_{34} \\ Y_{41} & Y_{42} & Y_{43} & Y_{44} \end{bmatrix} \begin{bmatrix} \phi \\ \overline{p} \\ v \\ w \end{bmatrix} + \begin{bmatrix} 0 & 0 \\ N_{21} & N_{22} \\ Y_{\theta_{1c}} & Y_{\theta_{0T}} \\ Z_{\theta_{1c}} & Z_{\theta_{0T}} \end{bmatrix} \begin{bmatrix} \theta_{1c} \\ \theta_{0T} \end{bmatrix}, \quad (18)$$

where

$$\begin{aligned} Y_{11} &= 0, \\ Y_{12} &= 1, \\ Y_{13} &= b_{11}, \\ Y_{14} &= b_{12}, \\ Y_{21} &= -(b_{11}g), \\ Y_{22} &= \left(L_p - b_{11}\left(Y_p + w_e\right) - b_{12}\left(Z_p - v_e\right)\right), \\ Y_{23} &= \left(L_p - b_{11}\left(Y_p + w_e\right) - b_{12}\left(Z_p - v_e\right)\right) b_{11} \\ &\quad + \left(L_p - b_{11}Y_v - b_{12}Z_v\right), \\ Y_{24} &= \left(L_p - b_{11}\left(Y_p + w_e\right) - b_{12}\left(Z_p - v_e\right)\right) b_{12} \\ &\quad + \left(L_p - b_{11}Y_w - b_{12}Z_w\right), \\ Y_{31} &= g, \\ Y_{32} &= \left(Y_p + w_e\right), \\ Y_{33} &= \left(\left(Y_p + w_e\right) b_{11} + Y_v\right), \\ Y_{34} &= \left(\left(Y_p + w_e\right) b_{12} + Y_w\right), \\ Y_{41} &= 0, \\ Y_{42} &= \left(Z_p - v_e\right), \\ Y_{43} &= \left(\left(Z_p - v_e\right) b_{11} + Z_v\right), \\ Y_{44} &= \left(\left(Z_p - v_e\right) b_{12} + Z_w\right), \\ N_{21} &= \left(L_{\theta_{1c}} - b_{11}Y_{\theta_{1c}} - b_{12}Z_{\theta_{1c}}\right), \\ N_{22} &= \left(L_{\theta_{0T}} - b_{11}Y_{\theta_{0T}} - b_{12}Z_{\theta_{0T}}\right). \end{aligned} \quad (19)$$

Using (18) the helicopter with underslung load for lateral motion in the $Y$-$Z$ plane can be described by

$$\begin{aligned} \dot{\overline{\varphi}}_L(t) &= f_1\left(\overline{\varphi}_L(t)\right) \\ &\quad + G_1\left(\overline{\varphi}_L(t)\right)\left[p\left(x_H(t)\right) + q\left(\overline{\varphi}_L(t), x_H(t)\right)\right] \\ &\quad + H\left(t, \overline{\varphi}_L, x_H(t)\right) \end{aligned} \quad (20a)$$

$$\dot{x}_H(t) = f_2\left(\overline{\varphi}_L(t), x_H(t)\right) + G_2\hat{u}(t), \quad (20b)$$

where

$$\begin{aligned} \dot{\overline{\varphi}}_L(t) &= \left[\dot{\varphi}_{L_1} \ \ \dot{\varphi}_{L_2} \ \ \dot{\phi} \ \ \dot{\overline{p}}\right]^T, \\ p\left(x_H(t)\right) &= \left[v^2 \ \ w^2\right]^T, \\ f_1\left(\overline{\varphi}_L(t)\right) &= \begin{bmatrix} \varphi_{L_2} \\ \dfrac{-g}{l_y}\sin\varphi_{L_1} + \dfrac{k_D l_y}{M_L}\left(\operatorname{sign}\left(\dot{Y}_L\right)\cos^3\varphi_{L_1} + \sin\left(\dot{Z}_L\right)\sin^3\varphi_{L_1}\right)\varphi_{L_2}^2 - k_\varphi\varphi_{L_2} \\ \overline{p} \\ \left(-b_{11}g\phi + \left(L_p - b_{11}\left(Y_p + w_e\right) - b_{12}\left(Z_p - v_e\right)\right)\overline{p}\right) \end{bmatrix}, \\ G_1\left(\overline{\varphi}_L(t)\right) &= \begin{bmatrix} 0 & 0 \\ \left(\dfrac{k_D \operatorname{sign}\left(\dot{Z}_L\right)\cos\varphi_{L_1}}{M_L l_y}\right) & \left(\dfrac{k_D \operatorname{sign}\left(\dot{Z}_L\right)\sin\varphi_{L_1}}{M_L l_y}\right) \\ 0 & 0 \\ 0 & 0 \end{bmatrix}, \\ q\left(\overline{\varphi}_L(t), x_H(t)\right) &= \begin{bmatrix} 0 \\ \dfrac{\cos\varphi_{L_1}}{l_y}\dot{v} + \dfrac{\sin\varphi_{L_1}}{l_y}\dot{w} - \dfrac{2k_D}{M_L}\left(\operatorname{sign}\left(\dot{Y}_L\right)\cos^2\varphi_{L_1} v + \operatorname{sign}\left(\dot{Z}_L\right)\sin^2\varphi_{L_1} w\right)\varphi_{L_2} \end{bmatrix}, \end{aligned}$$

$$H\left(t,\overline{\varphi}_L(t),x_H(t)\right)=\begin{bmatrix}0\\0\\\left(\dot{\phi}-\overline{p}\right)\\\left(Y_{23}v+Y_{24}w\right)\end{bmatrix},$$
$$\widehat{u}(t)=\left[\theta_{1c}\ \ \theta_{0T}\right]^T,$$
$$f_2\left(\overline{\varphi}_L(t),x_H(t)\right)=\begin{bmatrix}\left(Y_{31}\phi+Y_{32}\overline{p}+Y_{33}v+Y_{34}w\right)\\\left(Y_{42}\overline{p}+Y_{43}v+Y_{44}w\right)\end{bmatrix},$$
$$G_2=\begin{bmatrix}Y_{\theta_{1c}} & Y_{\theta_{0T}}\\Z_{\theta_{1c}} & Z_{\theta_{0T}}\end{bmatrix}. \tag{21}$$

It is assumed that the lateral motion is primarily controlled by lateral cyclic commands ($\theta_{1c}$) and the tail rotor collective $\theta_{0T}$.

## 3. Stability Analysis

The goal is to analyse the stability of the combined system to ensure that it is possible to stabilise the helicopter with underslung load system modelled by (11a), (11b), (20a), and (20b), in a real environment with uncertainties. In this paper, for the stability analysis the Lyapunov second method is applied for the helicopter with an underslung external load system. The analysis for the longitudinal motion is discussed first. The system equations can be considered to have two main parts, that is, known and unknown (or partly known). The known terms formed the nominal part of the system model. The unknown or partly known part can be considered as the uncertainty to the system. The whole system is then modelled by a nominal part with the addition of uncertainty. In fact, the known elements in the subsystem (11a) are characterised by the prescribed triple $(f_1, G_1, p)$ and it is desired that the nominal part of the system is stable.

The basic notations and concepts required for the analysis are described first. The state space is denoted by $X := \mathbb{R}^n$ and the control space by $\overline{u} := \mathbb{R}^m$, where $1 \le m \le n$. The Euclidean inner product (on $X$ or $\overline{u}$ as appropriate) and induced norm are denoted by $\langle\cdot,\cdot\rangle$ and $\|\cdot\|$, respectively. Let $C(\mathbb{R}^p;\mathbb{R}^q)$ and $C^1(\mathbb{R}^p;\mathbb{R}^q)$ denote the space of all continuous functions and the space of continuous functions with continuous first-order partial derivatives, respectively, and let $C^\infty(\mathbb{R}^p;\mathbb{R}^q)$ denote the space of functions whose partial derivatives of any order exist and are continuous, mapping $\mathbb{R}^p \to \mathbb{R}^q$. For a real-valued continuous scalar function $x \to v(x)$, defined on $\mathbb{R}^n, \nabla : \widetilde{v} \to \nabla\widetilde{v} \in \mathbb{R}^n$ denotes the gradient map. The Lie derivative of $v$ along a vector field $f : \mathbb{R}^n \to \mathbb{R}^n$ is denoted by $L_f\widetilde{v} : \mathbb{R}^n \to \mathbb{R}$ which is defined by

$$\left(L_f\widetilde{v}\right)(x)=\left\langle\nabla\widetilde{v}(x), f(x)\right\rangle. \tag{22}$$

The Lie bracket of vector fields $f, g \in C^\infty(\mathbb{R}^n,\mathbb{R}^n)$ is the vector field $[f,g] \in C^\infty(\mathbb{R}^n,\mathbb{R}^n)$ defined by $[f,g] = (Dg)f - (Df)g$, where $(Df)$ denotes the Jacobian matrix of $f$ and $(Dg)$ denotes the Jacobian matrix of $g$.

In this paper, nonlinear systems with the following format are considered:

$$\dot{x}(t)=f(x(t))+G(x(t))\widetilde{u}(t), \tag{23}$$

where $x(t) \in \mathbb{R}^n$, $\widetilde{u} \in \mathbb{R}^m$. In general mathematical models of dynamical systems are usually imprecise due to modelling errors and exogenous disturbances [12]. Equation (23) can be considered as the nominal part of the system model and the uncertainty can be modelled as an additive perturbation to the nominal system model; more specifically, the structure of the system has the form

$$\dot{x}(t)=f(x(t))+G(x(t))\widetilde{u}(t)+\vartheta(x(t),u(t)), \tag{24}$$

where $\vartheta(x(t),u(t))$ models the uncertainty in the system.

System (24) is globally asymptotically stable to the zero state if the system exhibits the following properties.

*(i) Existence and Continuation of Solutions*. For each $x \in \mathbb{R}^n$, there exists a local solution $x : [0,t_1) \to \mathbb{R}^n$ (i.e., an absolutely continuous function satisfying (24) almost everywhere (a.e.) and $x(0) = x^0$) and every such solution can be extended into a solution on $[0,\infty)$.

*(ii) Boundedness of Solutions*. For each $\hbar > 0$, there exists $r(\hbar) > 0$ such that $x(t) \in r(\hbar)B_n$, for all $t \ge 0$ on every solution $x : [0,\infty) \to \mathbb{R}^n$ with $x^0 \in \hbar B_n$, where $B_n$ denote the open unit ball centred at the origin in $\mathbb{R}^n$.

*(iii) Stability of the State Origin*. For each $\delta > 0$, there exists $d(\delta) > 0$ such that $x(t) \in \delta B_n$ for all $t \ge 0$ on every solution $x : [0,\infty) \to \mathbb{R}^n$ with $x^0 \in d(\delta)B_n$.

*(iv) Global Attractivity of the State Origin*. For each $\hbar > 0$ and $\varepsilon > 0$, there exists $T(\hbar,\varepsilon) \ge 0$ such that $x(t) \in B_n$ for all $t \ge T(\hbar,\varepsilon)$ on every solution $x : [0,\infty) \to \mathbb{R}^n$ with $x^0 \in \hbar B_n$.

Consider a nonlinear system described by the ordinary differential equation as follows:

$$\dot{x}(t) = f(t, x(t)), \quad x(t_0) = x^0, \tag{25}$$

where $f : \mathbb{R} \times X \to X$ and $f(t, 0) = 0$ for all $t$. To analyse the stability of (25), Lyapunov's second stability analysis method is applicable. The Lyapunov approach is to show that a candidate "Lyapunov function" is nonincreasing along all solution to (25) by means that do not require explicit knowledge of solutions to (25). From this, appropriate conclusion can be drawn regarding stability concepts relating to solutions of the differential equation (25). An essential part of Lyapunov's method is the determination of the time derivative of the candidate "Lyapunov function" along all solution of the dynamical system.

Consider a Lyapunov candidate $(t, x) \to \tilde{v}(t, x) : \mathbb{R}\times X \to \mathbb{R}$ which satisfies the condition $\tilde{v} \in C^1(\mathbb{R} \times X)$, in which case its time derivative along solutions to (25) is given by

$$\dot{v}(t, x(t)) = \frac{\partial \tilde{v}(t, x(t))}{\partial t} + \langle \nabla \tilde{v}(t, x(t)), f(t, x(t)) \rangle \tag{26}$$

for almost all $t \in \mathbb{R}$.

Let $W(x(t))$ denote a positive definite function. If $\tilde{v}(t, x(t))$ satisfies

(i) $\tilde{v}(t, 0) = 0$ for all $t \geq 0$,

(ii) $W(x(t)) \leq \tilde{v}(t, x(t))$ for all $x(t) \in \Phi$, $\{0\} \subset \Phi \subset X$ and all $t \geq 0$,

(iii) $\dot{v}(t, x(t)) < 0$ in $\Phi$,

then $\tilde{v}(t, x(t))$ is said to be a Lyapunov function in $\Phi$. If $\dot{\tilde{v}}(t, x(t))$ in $\Phi$, then $\tilde{v}(t, x(t))$ is said to be a weak Lyapunov function.

A set E is said to be an invariant set with respect to the dynamical system $\dot{x} = f(x)$ if

$$x(0) \in \mathrm{E} \longmapsto x(t) \in \mathrm{E} \quad \forall t \in \mathbb{R}^+. \tag{27}$$

In other words E is the set of points such that if a solution of $\dot{x} = f(x)$ belongs to E at some instant initialized points at $t = 0$, then it belongs to E for all future time.

Now, a set $\mathrm{E} \subset x$ is said to be a local invariant manifold for (25) if, for any $x^0 \in \mathrm{E}$, $x(t)$ with $x(0) = x^0$ is in E for $|t| < T$ where $T > 0$. If $T = \infty$, then E is said to be an invariant manifold.

Now considering the longitudinal motion (Figure 1) for the helicopter with an underslung external load system, choose a Lyapunov function candidate for the first subsystem $v_1$ as

$$v_1(\overline{\theta}_L) = \frac{1}{2}\left[\varsigma_1\theta_{L_1}^2 + \varsigma_2\theta_{L_2}^2 + (\varsigma_3\theta - \varsigma_4\overline{q})^2 + \varsigma_5\overline{q}^2\right], \tag{28}$$

where $\varsigma_i$ $(i = 1, 2, 3, 4, 5)$ are design parameters to be determined. Then

$$\begin{aligned}\dot{v}_1(\overline{\theta}_L) &= \langle \nabla v_1(\overline{\theta}_L), f_1(\overline{\theta}_L) + G_1(\overline{\theta}_L(t)) \\ &\quad \cdot [p(x_H(t)) + q(\overline{\theta}_L(t), x_H(t))] \\ &\quad + H(t, \overline{\theta}_L, x_H(t)) \rangle = (L_{f_1}v_1)(\overline{\theta}_L) \\ &\quad + \langle \nabla v_1(\overline{\theta}_L), G_1(\overline{\theta}_L(t)) \\ &\quad \cdot [p(x_H(t)) + q(\overline{\theta}_L(t), x_H(t))] \\ &\quad + H(t, \overline{\theta}_L, x_H(t)) \rangle.\end{aligned} \tag{29}$$

From (28), $\nabla v_1(\overline{\theta}_L)$ can be obtained as

$$\begin{aligned}&\nabla v_1(\overline{\theta}_L) \\ &= [\varsigma_1\theta_{L_1} \quad \varsigma_2\theta_{L_2} \quad \varsigma_3(\varsigma_3\theta - \varsigma_4\overline{q}) \quad -\varsigma_4(\varsigma_3\theta - \varsigma_4\overline{q}) + \varsigma_5\overline{q}]^T.\end{aligned} \tag{30}$$

Substituting $\nabla v_1(\overline{\theta}_L)$ and $f_1(\overline{\theta}_L)$ into the derivative of $(L_{f_1}v_1)(\overline{\theta}_L)$, we have

$$\begin{aligned}(L_{f_1}v_1)(\overline{\theta}_L) &= \varsigma_1\theta_{L_1}\theta_{L_2} - k_\theta\varsigma_2\theta_{L_2}^2 - \varsigma_2\frac{g}{l_x}\sin\theta_{L_1}\theta_{L_2} \\ &\quad + \frac{k_D l_x}{M_L}\varsigma_2\left[\mathrm{sign}(\dot{X}_L)\cos^3\theta_{L_1} + \mathrm{sign}(\dot{Z}_L)\sin^3\theta_{L_1}\right] \\ &\quad \cdot \theta_{L_2}^3 + \varsigma_3[\varsigma_3\theta - \varsigma_4\overline{q}]\overline{q} + \left(-\varsigma_3\varsigma_4\theta + (\varsigma_4^2 + \varsigma_5)\overline{q}\right) \\ &\quad \cdot [X_{21}\theta + X_{22}\overline{q}].\end{aligned} \tag{31}$$

Checking the term of $-\sin(\theta_{L_1})\theta_{L_2}$, it can be seen that $-\sin(\theta_{L_1})\theta_{L_2} \leq -(2/\pi)\theta_{L_1}\theta_{L_2}$ when $\theta_{L_1}$ and $\theta_{L_2}$ are both positive or negative. The situation of $\theta_{L_1}$ and $\theta_{L_2}$ having different signs will help with the system stability. Then,

$$\begin{aligned}(L_{f_1}v_1)(\overline{\theta}_L) &\leq \varsigma_1\theta_{L_1}\theta_{L_2} - k_\theta\varsigma_2\theta_{L_2}^2 - \varsigma_2\frac{g}{l_x}\frac{2}{\pi}\theta_{L_1}\theta_{L_2} \\ &\quad + \frac{k_D l_x}{M_L} \\ &\quad \cdot \varsigma_2\left[\mathrm{sign}(\dot{X}_L)\cos^3\theta_{L_1} + \mathrm{sign}(\dot{Z}_L)\sin^3\theta_{L_1}\right]\theta_{L_2}^3 \\ &\quad + \varsigma_3[\varsigma_3\theta - \varsigma_4\overline{q}]\overline{q} + \left(-\varsigma_3\varsigma_4\theta + (\varsigma_4^2 + \varsigma_5)\overline{q}\right) \\ &\quad \cdot [X_{21}\theta + X_{22}\overline{q}].\end{aligned} \tag{32}$$

If the design parameter $\varsigma_1$ is chosen as $\varsigma_1 = (2g/l_x\pi)\varsigma_2$, $(L_{f_1}v_1)(\overline{\theta}_L)$ satisfies the following:

$$\begin{aligned}(L_{f_1}v_1)(\overline{\theta}_L) &\leq -k_\theta\varsigma_2\theta_{L_2}^2 + \frac{k_D l_x}{M_L} \\ &\quad \cdot \varsigma_2\left[\mathrm{sign}(\dot{X}_L)\cos^3\theta_{L_1} + \mathrm{sign}(\dot{Z}_L)\sin^3\theta_{L_1}\right]\theta_{L_2}^3 \\ &\quad + \varsigma_3[\varsigma_3\theta - \varsigma_4\overline{q}]\overline{q} + \left(-\varsigma_3\varsigma_4\theta + (\varsigma_4^2 + \varsigma_5)\overline{q}\right) \\ &\quad \cdot [X_{21}\theta + X_{22}\overline{q}].\end{aligned} \tag{33}$$

Further analysis on (33) will start from examining the first two terms. Rewrite these two terms. So

$$\begin{aligned}&-k_\theta\varsigma_2\theta_{L_2}^2+\frac{k_Dl_x}{M_L}\varsigma_2\left[\operatorname{sign}\left(\dot{X}_L\right)\cos^3\theta_{L_1}+\operatorname{sign}\left(\dot{Z}_L\right)\right.\\&\left.\cdot\sin^3\theta_{L_1}\right]\theta_{L_2}^3=-k_\theta\varsigma_2\theta_{L_2}^2+\frac{k_Dl_x}{M_L}\varsigma_2\theta_{L_2}\left[\operatorname{sign}\left(\dot{X}_L\right)\right.\\&\left.\cdot\cos^3\theta_{L_1}+\operatorname{sign}\left(\dot{Z}_L\right)\sin^3\theta_{L_1}\right]\theta_{L_2}^2\le-k_\theta\varsigma_2\theta_{L_2}^2\\&+\frac{k_Dl_x}{M_L}\varsigma_2\left|\max\left(\theta_{L_2}\right)\left(\operatorname{sign}\left(\dot{X}_L\right)\cos^3\theta_{L_1}\right.\right.\\&\left.\left.+\operatorname{sign}\left(\dot{Z}_L\right)\sin^3\theta_{L_1}\right)\right|\theta_{L_2}^2=-\varsigma_2\theta_{L_2}^2\left\{k_\theta\right.\\&-\frac{k_Dl_x}{M_L}\left|\max\left(\theta_{L_2}\right)\right.\\&\left.\left.\cdot\left(\operatorname{sign}\left(\dot{X}_L\right)\cos^3\theta_{L_1}+\operatorname{sign}\left(\dot{Z}_L\right)\sin^3\theta_{L_1}\right)\right|\right\}.\end{aligned}\tag{34}$$

If the hinge friction is big enough to satisfy the following:

$$\begin{aligned}k_\theta&>\frac{k_Dl_x}{M_L}\left|\max\left(\theta_{L_2}\right)\right.\\&\left.\cdot\left(\operatorname{sign}\left(\dot{X}_L\right)\cos^3\theta_{L_1}+\operatorname{sign}\left(\dot{Z}_L\right)\sin^3\theta_{L_1}\right)\right|,\end{aligned}\tag{35}$$

then

$$\begin{aligned}\lambda_L&=\left\{k_\theta-\frac{k_Dl_x}{M_L}\left|\max\left(\theta_{L_2}\right)\right.\right.\\&\left.\left.\cdot\left(\operatorname{sign}\left(\dot{X}_L\right)\cos^3\theta_{L_1}+\operatorname{sign}\left(\dot{Z}_L\right)\sin^3\theta_{L_1}\right)\right|\right\}\ge0,\\&-k_\theta\varsigma_2\theta_{L_2}^2+\frac{k_Dl_x}{M_L}\varsigma_2\left[\operatorname{sign}\left(\dot{X}_L\right)\cos^3\theta_{L_1}+\operatorname{sign}\left(\dot{Z}_L\right)\right.\\&\left.\cdot\sin^3\theta_{L_1}\right]\theta_{L_2}^3\le-\varsigma_2\theta_{L_2}^2\lambda_L.\end{aligned}\tag{36}$$

Now, the following analysis has been conducted for (33) and the load movement for the longitudinal motion is described by

$$\begin{aligned}\dot{X}_L&=\dot{X}_0-l_x\theta_{L_2}\cos\theta_{L_1}\\\dot{Z}_L&=\dot{Z}_0-l_x\theta_{L_2}\sin\theta_{L_1}.\end{aligned}\tag{37}$$

Around the hover condition $X_0=0$ and $Z_0=0$, the signs for $\dot{X}_L$ and $\dot{Z}_L$ are opposite to the one of $\theta_{L_2}$ provided that $\theta_{L_1}$ is positive.

Considering the term $(\operatorname{sign}(\dot{X}_L)\cos^3\theta_{L_1}+\operatorname{sign}(\dot{Z}_L)\sin^3\theta_{L_1})\theta_{L_2}^3$ for all possible combinations of the signs of $\theta_{L_2}$ and $\theta_{L_1}$, the analysis follows below:

(i) If $\theta_{L_1}>0$ and $\theta_{L_2}>0$, then $\operatorname{sign}(\dot{X}_L)=-1$, $\operatorname{sign}(\dot{Z}_L)=-1$, $\cos^3\theta_{L_1}>0$, and $\sin^3\theta_{L_1}>0$. Therefore, $(\operatorname{sign}(\dot{X}_L)\cos^3\theta_{L_1}+\operatorname{sign}(\dot{Z}_L)\sin^3\theta_{L_1})\theta_{L_2}^3<0$.

(ii) If $\theta_{L_1}<0$ and $\theta_{L_2}>0$, then $\operatorname{sign}(\dot{X}_L)=-1$, $\operatorname{sign}(\dot{Z}_L)=+1$, $\cos^3\theta_{L_1}>0$, and $\sin^3\theta_{L_1}<0$. So $(\operatorname{sign}(\dot{X}_L)\cos^3\theta_{L_1}+\operatorname{sign}(\dot{Z}_L)\sin^3\theta_{L_1})\theta_{L_2}^3<0$.

(iii) If $\theta_{L_1}>0$ and $\theta_{L_2}<0$, then $\operatorname{sign}(\dot{X}_L)=+1$ and $\operatorname{sign}(\dot{Z}_L)=+1$, $\cos^3\theta_{L_1}>0$, and $\sin^3\theta_{L_1}>0$. So the following is true: $(\operatorname{sign}(\dot{X}_L)\cos^3\theta_{L_1}+\operatorname{sign}(\dot{Z}_L)\sin^3\theta_{L_1})\theta_{L_2}^3<0$.

(iv) If $\theta_{L_1}<0$ and $\theta_{L_2}<0$, then $\operatorname{sign}(\dot{X}_L)=+1$ and $\operatorname{sign}(\dot{Z}_L)=-1$, $\cos^3\theta_{L_1}>0$, and $\sin^3\theta_{L_1}<0$. So $(\operatorname{sign}(\dot{X}_L)\cos^3\theta_{L_1}+\operatorname{sign}(\dot{Z}_L)\sin^3\theta_{L_1})\theta_{L_2}^3<0$.

Therefore

$$\begin{aligned}&-k_\theta\varsigma_2\theta_{L_2}^2+\frac{k_Dl_x}{M_L}\\&\quad\cdot\varsigma_2\left[\operatorname{sign}\left(\dot{X}_L\right)\cos^3\theta_{L_1}+\operatorname{sign}\left(\dot{Z}_L\right)\sin^3\theta_{L_1}\right]\theta_{L_2}^3\\&\quad\le-k_\theta\varsigma_2\theta_{L_2}^2.\end{aligned}\tag{38}$$

Now examining the rest of the terms of $(L_{f_1}\nu_1)(\overline{\theta}_L)$, then

$$\begin{aligned}&\varsigma_3\left[\varsigma_3\theta-\varsigma_4\overline{q}\right]\overline{q}\\&\quad+\left(-\varsigma_3\varsigma_4\theta+\left(\varsigma_4^2+\varsigma_5\right)\overline{q}\right)\left[X_{21}\theta+X_{22}\overline{q}\right]=\varsigma_3^2\theta\overline{q}\\&\quad-\varsigma_3\varsigma_4\overline{q}^2-\varsigma_3\varsigma_4X_{21}\theta^2-\varsigma_3\varsigma_4X_{22}\theta\overline{q}\\&\quad+\left(\varsigma_4^2+\varsigma_5\right)X_{21}\theta\overline{q}+\left(\varsigma_4^2+\varsigma_5\right)X_{22}\overline{q}^2\\&\quad=-\left[\varsigma_3\varsigma_4-\left(\varsigma_4^2+\varsigma_5\right)X_{21}\right]\overline{q}^2-\varsigma_3\varsigma_4X_{21}\theta^2\\&\quad+\left[\varsigma_3^2-\varsigma_3\varsigma_4X_{22}+\left(\varsigma_4^2+\varsigma_5\right)X_{21}\right]\theta\overline{q}.\end{aligned}\tag{39}$$

For the system, $\theta$ and $\theta_{L_1}$ always have different signs, $\theta$ and $\overline{q}$ always have different signs, and $\overline{q}$ and $\theta_{L_1}$ have the same signs. So

$$\begin{aligned}&\left[\varsigma_3^2-\varsigma_3\varsigma_4X_{22}+\left(\varsigma_4^2+\varsigma_5\right)X_{21}\right]\theta\overline{q}\le0\\&\text{if }\left[\varsigma_3^2-\varsigma_3\varsigma_4X_{22}+\left(\varsigma_4^2+\varsigma_5\right)X_{21}\right]\ge0.\end{aligned}\tag{40}$$

Therefore

$$\begin{aligned}&\varsigma_3\left[\varsigma_3\theta-\varsigma_4\overline{q}\right]\overline{q}\\&\quad+\left(-\varsigma_3\varsigma_4\theta+\left(\varsigma_4^2+\varsigma_5\right)\overline{q}\right)\left[X_{21}\theta+X_{22}\overline{q}\right]\\&\quad\le-\left[\varsigma_3\varsigma_4-\left(\varsigma_4^2+\varsigma_5\right)X_{21}\right]\overline{q}^2-\varsigma_3\varsigma_4X_{21}\theta^2.\end{aligned}\tag{41}$$

Choose the design parameters to satisfy

$$\left[\varsigma_3\varsigma_4-\left(\varsigma_4^2+\varsigma_5\right)X_{21}\right]>0.\tag{42}$$

If $X_{21}>0$, then

$$-\left[\varsigma_3\varsigma_4-\left(\varsigma_4^2+\varsigma_5\right)X_{21}\right]\overline{q}^2-\varsigma_3\varsigma_4X_{21}\theta^2<0.\tag{43}$$

If $X_{21} < 0$, then

$$-\left[\varsigma_3\varsigma_4 - \left(\varsigma_4^2 + \varsigma_5\right) X_{21}\right] \bar{q}^2 - \varsigma_3\varsigma_4 X_{21}\theta^2 < 0 \quad (44)$$

in the region of $-[\varsigma_3\varsigma_4-(\varsigma_4^2+\varsigma_5)X_{21}]\bar{q}^2 < \varsigma_3\varsigma_4X_{21}\theta^2$. Since $\theta$ is caused by the load motion here the value of $\theta$ should be much smaller than $\bar{q}$. The inequality (44) is easy to be satisfied.

In summary of the above analysis and by defining

$$\begin{aligned}\Psi_1\left(\bar{\theta}_L\right) &= k_\theta\varsigma_2\theta_{L_2}^2 + \left[\varsigma_3\varsigma_4 - \left(\varsigma_4^2 + \varsigma_5\right) X_{21}\right] \bar{q}^2 \\ &\quad + \varsigma_3\varsigma_4 X_{21}\theta^2, \\ \Psi_2\left(\bar{\theta}_L\right) &= \left[\varsigma_3\varsigma_4 - \left(\varsigma_4^2 + \varsigma_5\right) X_{21}\right] \bar{q}^2 + \varsigma_3\varsigma_4 X_{21}\theta^2,\end{aligned} \quad (45)$$

the following lemma can be derived.

**Lemma 1.** *Defining a Lyapunov function (28) and choosing the design parameters to satisfy* $\varsigma_1 = (2g/l_x\pi)\varsigma_2$, $[\varsigma_3\varsigma_4 - (\varsigma_4^2 + \varsigma_5)X_{21}] > 0$, *and* $[\varsigma_3^2 - \varsigma_3\varsigma_4X_{22} + (\varsigma_4^2+\varsigma_5)X_{21}] \geq 0$, *then within the region specified by* $-[\varsigma_3\varsigma_4 - (\varsigma_4^2 + \varsigma_5)X_{21}]\bar{q}^2 < \varsigma_3\varsigma_4X_{21}\theta^2$

(i) $v_1(0) = 0$ *and* $v_1(\bar{\theta}_L) > 0$, $\forall\bar{\theta}_L \neq 0$,

(ii) $v_1(\bar{\theta}_L) \to \infty$ *as* $\|\bar{\theta}_L\| \to \infty$,

(iii) $(L_{f_1}v_1)(\bar{\theta}_L) \leq -\Psi_1(\bar{\theta}_L)$, $\forall\bar{\theta}_L$, *around the hover condition or* $(L_{f_1}v_1)(\bar{\theta}_L) \leq -\Psi_2(\bar{\theta}_L)$, $\forall\bar{\theta}_L$, *if (35) holds.*

Both functions $\Psi_1$ and $\Psi_2$ are nonnegative.

Recall the control term $p(x_H(t))$ in the first subsystem of (11a) and (11b); it can be seen that $[(Dp)(x_H)]^{-1}$ exists for all $x_H(t)$. The unknown vector fields, $q(\bar{\theta}_L(t), x_H)$ and $H(t,\bar{\theta}_L(t), x_H)$, model the uncertainties imposed onto the system. Since $q(\bar{\theta}_L(t), x_H)$ is directly mapped into the "control" space of $x_H(t)$ it can be considered as a matched uncertainty. $H(t,\bar{\theta}_L(t), x_H)$ is unknown and it does belong to the control space of $x_H(t)$; so it represents the mismatched uncertainty in the system [12].

Generally, the range of the (longitudinal) load suspension angle is within $-\pi/2 < \theta_L < \pi/2$. The helicopter velocities and load suspension angle have maximum operational values; therefore the uncertainties in the system are bounded. With the Lyapunov function defined in (28),

$$\left(L_{g_1}v_1\right)\left(\bar{\theta}_L\right) = \left\langle \nabla v_1\left(\bar{\theta}_L\right), g_1\right\rangle = \frac{k_D}{M_L l_x}\varsigma_2\theta_{L_2}. \quad (46)$$

In $G_1(\bar{\theta}_L)$ the columns $g_1$ and $g_2$ are the same; therefore

$$\left(L_{g_2}v_1\right)\left(\bar{\theta}_L\right) = \frac{k_D}{M_L l_x}\varsigma_2\theta_{L_2}. \quad (47)$$

By considering the maximum values of $\cos(\cdot)$ and $\sin(\cdot)$ functions, the bounding values relating to the uncertainty $q(\bar{\theta}_L(t), x_H)$ can be estimated as follows:

$$\begin{aligned}\left\|q\left(\bar{\theta}_L, x_H\right)\right\| &\leq \left|\frac{1}{l_x}(\dot{u}+\dot{w}) + \frac{1}{M_L}\left(-k_D\left(2+\frac{\kappa}{l_x}\right)(u+w) + \frac{k_\theta}{l_x}\right)\bar{\theta}_{L_2}\right| \\ &\leq \left|\frac{k_\theta}{l_x}\theta_{L_2}\right| + \left|\frac{k_D}{M_L}\left(2+\frac{\kappa}{l_x}\right)(u+w)\right| + \left|\frac{1}{l_x}(\dot{u}+\dot{w})\right| \\ &\leq \frac{k_\theta}{l_x}\left\|\theta_{L_2}\right\| + \frac{k_D}{M_L}\left(2+\frac{\kappa}{l_x}\right)\left\|p\left(x_H\right)\right\| + \alpha_2(t) \\ &\leq \mu_1\left|\left(L_{g_2}v_1\right)\left(\bar{\theta}_L\right)\right| + \alpha_1\left\|p\left(x_H\right)\right\| + \alpha_2(t),\end{aligned} \quad (48)$$

where $\mu_1 = M_Lk_\theta/k_D$, $\alpha_1 = (k_D/M_L)(2 + \kappa/l_x)$ ($\kappa = \max[\kappa_1 \ \ \kappa_2]$), and $\alpha_2(t)$ is defined by $\alpha_2(t) = \max|(1/l_x)(\dot{u} + \dot{w})| > 0$.

For the mismatched uncertainty $H(t,\bar{\theta}_L(t), x_H)$ the following analysis is conducted to obtain its bounding function. The mismatched uncertainty can be rewritten as

$$H\left(t,\bar{\theta}_L(t), x_H\right) = \begin{bmatrix} 0 \\ 0 \\ (a_{11}u + a_{12}w) \\ (X_{23}u + X_{24}w) \end{bmatrix} = \begin{bmatrix} 0 & 0 \\ 0 & 0 \\ a_{11} & a_{12} \\ X_{23} & X_{24} \end{bmatrix}\begin{bmatrix} u \\ w \end{bmatrix}. \quad (49)$$

Let $\bar{A} = \left[\begin{smallmatrix} a_{11} & a_{12} \\ X_{23} & X_{24} \end{smallmatrix}\right]$; then

$$\left\|H\left(t,\bar{\theta}_L, x_H\right)\right\| \leq \left\|\bar{A}\right\| \left\|x_H(t)\right\|. \quad (50)$$

Define a positive function as

$$\bar{\theta}\left(\bar{\theta}_L\right) = \sqrt{\left(\theta_{L_1}^2 + \theta_{L_2}^2 + \theta^2 + \bar{q}^2 + \bar{\varepsilon}\right)}, \quad (51)$$

where $\bar{\varepsilon}$ is a very small positive constant. Choosing $\beta_1 = (M_Ll_x/k_D\varsigma_2)\|\bar{A}\|$ then the mismatched uncertainty $H(t,\bar{\theta}_L(t), x_H)$ is bounded by the following inequality:

$$\begin{aligned}&\left\|H\left(t,\bar{\theta}_L, x_H\right)\right\| \\ &\quad \leq \bar{\theta}^{-1}\left(\bar{\theta}_L\right)\beta_1\sum_{i=1}^{2}\left(\left|\left(L_{g_i}v_1\right)\left(\bar{\theta}_L\right)\right|\right)\left|p_i\left(x_H\right)\right|,\end{aligned} \quad (52)$$

where $g_i$ denotes the $i$th column of the matrix function $G_1(\bar{\theta}_L)$ and $p_i$ is the $i$th component of $p(x_H)$, respectively. As $\beta_1$ has a design parameter $\varsigma_2$ involved it is easy to have $\beta_1$ to lead (52) to be true. For the matched uncertainty, we have

$$\left\|q\left(\bar{\theta}_L, x_H\right)\right\| \leq \frac{k_\theta}{l_x}\left|\theta_{L_2}\right| + \alpha_1\left\|p\left(x_H\right)\right\| + \alpha_2(t). \quad (53)$$

Following the above analysis, the following lemma can be derived.

**Lemma 2.** *The uncertainties (52) and (53) are bounded and satisfy, if* $\alpha_1$, $\beta_1 \geq 0$, *and* $\alpha_1 + \beta_1 < 1$, *for* $\alpha_1 = (k_D/M_L)(2 + \kappa/l_x)$ *and* $\beta_1 = (M_L l_x/k_D\varsigma_2)\|\overline{A}\|$.

## 4. Numerical Results

Using a simulation software the linearized model for a UH-60 helicopter is obtained with the following state and input matrices:

$$A = \begin{bmatrix} -0.0000 & 0.0003 & -0.0000 & -0.0000 & 0.0000 & -0.0000 & 1.0000 & -0.0023 & 0.0503 \\ -0.0003 & -0.0000 & -0.0000 & -0.0000 & -0.0000 & -0.0000 & -0.0000 & 0.9989 & 0.0463 \\ -0.0001 & 0.0000 & -0.0000 & -0.0000 & 0.0000 & 0.0000 & -0.0000 & -0.0464 & 1.0002 \\ -1.9386 & -28.593 & -0.0030 & -0.0195 & -0.0126 & 0.0168 & -1.2000 & 5.7076 & 0.2683 \\ 32.8694 & -0.3640 & 0.0027 & 0.0126 & -0.0311 & -0.0013 & -4.1348 & -2.2350 & 0.3713 \\ 0.3138 & -1.4034 & 0.0004 & 0.0150 & 0.0034 & -0.3340 & 0.2866 & 0.6307 & 2.3410 \\ -0.9144 & -0.4783 & 0.0017 & 0.0226 & -0.0246 & 0.0007 & -6.5893 & -2.1301 & -0.0598 \\ 0.0631 & -0.6744 & 0.0008 & 0.0029 & 0.0046 & 0.0025 & 0.2059 & -1.4255 & -0.1636 \\ -0.7549 & -0.0119 & -0.0002 & 0.0009 & 0.0028 & 0.0006 & -0.0749 & -0.1032 & -0.2214 \end{bmatrix}$$

$$B = \begin{bmatrix} -0.0000 & 0.0000 & -0.0000 & 0.0000 \\ 0.0000 & 0.0000 & -0.0000 & -0.0000 \\ -0.0000 & 0.0000 & -0.0000 & -0.0000 \\ -2.2190 & 0.5734 & 0.3170 & -0.0019 \\ 3.5381 & -0.0453 & -0.0963 & 0.2007 \\ -1.5629 & 0.0237 & -6.0740 & -0.1014 \\ 1.9943 & -0.0714 & -0.0541 & 0.0731 \\ 0.0446 & -0.1097 & 0.0553 & -0.0281 \\ -0.8197 & -0.0082 & 0.1573 & -0.0635 \end{bmatrix}. \quad (54)$$

The desired condition $\alpha_1 + \beta_1 < 1$ can be verified by considering a typical case that the UH-60 helicopter carries a load weight 1000 lb by a 15 ft slung length, and let $k_D = 75$ lb/ft.

For the UH-60 helicopter model, with reference to the general mathematical model presented in Section 2, we have $X_{\theta_{1s}} = 0.5734$, $X_{\theta_0} = 0.3170$, $Z_{\theta_{1s}} = 0.0237$, $Z_{\theta_0} = -6.0740$, $M_{\theta_{1s}} = -0.1097$, and $M_{\theta_0} = 0.0553$. So the following parameters can be calculated to have the values $a_{11} = -0.2$ and $a_{12} = -0.02$. For $X_u = -0.0195$, $Z_u = 0.0150$, $M_u = 0.0029$, $M_q = -1.4255$, $(X_q - w_e) = 5.7076$, and $(Z_q + u_e) = 0.6307$, we have $X_{23} = 0.06$. And also, for $X_w = 0.0168$, $Z_w = -0.3340$, and $M_w = 0.0025$, we have $X_{24} = 0.01$. Based on all the above parameters, $\sigma_{\max}(\overline{A}) = 0.0041$. In this case, let $\kappa = 0.01$, $\alpha_1 = (k_D/M_L)(2 + \kappa/l_x) \approx 0.15$, and $\beta_1 = (M_L l_x/k_D)\sigma_{\max}(\overline{A}) = 0.82$. Therefore, $\alpha_1 + \beta_1 = 0.15 + 0.82 = 0.97$ which satisfies $\alpha_1 + \beta_1 < 1$. Another example considers that the UH-60 helicopter carries a load weight 500 lb by a 15 ft slung length and let $k_D = 50$ lb/ft; then $\alpha_1 = 0.2$ and $\beta_1 = 0.62$; therefore $(\alpha_1 + \beta_1) = 0.82$. Therefore, this assumption $\alpha_1 + \beta_1 < 1$ is realistic for the system discussed in here. The numerical values vary with respect to the slung load configuration. It may represent the system dynamic variations. To investigate the stability characteristics of dynamic variations two series of simulation studies were carried out.

Firstly, the slung length was kept constant at 15 ft and the load varied between the limits 500–2000 lb with $k_D = 75$ lb/ft, producing the system poles listed in Table 1. The corresponding root loci are sketched in Figures 3 and 4. Figure 4 clearly shows that the positions of the system poles crossed the imaginary axis as the load weight increased.

Secondly, load weight was kept constant and the slung length varied between the limit of 10–20 ft. Table 2 summarises the results of variation of the system poles and the corresponding root loci are illustrated in Figures 5 and 6.

The pole locus indicates that the system poles have the variation trends of moving further towards right direction on the $s$-plane with increase of load weight and slung lengths. From the simulation results it is clearly shown that the system becomes less stable when the load and/or the slung length increases. The simulation results are compared with the stability analysis presented above.

Now, consider the case of fixed slung length of 15 ft with different load weights. In the cases of a UH-60 helicopter that

TABLE 1: System poles locations for a fixed slung length ($l$ = 15 ft) but with different load weights.

| Helicopter | 500 lb | 1000 lb | 1500 lb | 2000 lb |
|---|---|---|---|---|
| −1.0919 | −1.1159 | −0.7848 | −0.6221 | −0.9369 |
| −6.3938 | −6.4301 | −9.2203 | −7.9848 | −7.5613 |
| −0.0032 | −0.0048 | −0.0034 | −0.0052 | −0.0052 |
| −0.0977 | −0.0818 | −0.0888 | −0.0972 | −0.0694 |
| −0.3045 | −0.3036 | −0.3394 | −0.3318 | −0.3333 |
| $-0.3159 \pm 0.4363i$ | $-0.3199 \pm 0.4628i$ | $-0.2295 \pm 0.5050i$ | $-0.2366 \pm 0.5974i$ | $-0.1834 \pm 0.4968i$ |
| $-0.0489 \pm 0.3898i$ | $-0.0211 \pm 0.3868i$ | $0.0074 \pm 0.3445i$ | $0.0119 \pm 0.4406i$ | $0.0264 \pm 0.3199i$ |
| — | $-0.0316 \pm 1.5043i$ | $-0.1020 \pm 1.7380i$ | $-0.0368 \pm 1.8753i$ | $-0.1160 \pm 2.0003i$ |
| — | $-0.0736 \pm 1.5019i$ | $-0.7662 \pm 1.1680i$ | $-0.7349 \pm 1.9064i$ | $-1.2367 \pm 0.8995i$ |

TABLE 2: System poles for a fixed load (1000 lb) but with different slung lengths.

| Helicopter | 10 ft | 15 ft | 20 ft |
|---|---|---|---|
| −1.0919 | −1.0560 | −0.7848 | −0.8687 |
| −6.3938 | −9.9252 | −9.2203 | −8.5565 |
| −0.0032 | −0.0061 | −0.0034 | −0.0114 |
| −0.0977 | −0.2012 | −0.0888 | −0.0953 |
| −0.3045 | −0.2606 | −0.3394 | −0.3479 |
| $-0.3159 \pm 0.4363i$ | $-0.1809 \pm 0.6219i$ | $-0.2295 \pm 0.5050i$ | $-0.1636 \pm 0.6092i$ |
| $-0.0489 \pm 0.3898i$ | $0.0643 \pm 0.4577i$ | $0.0074 \pm 0.3445i$ | $0.0799 \pm 0.4594i$ |
| — | $-0.1055 \pm 1.9883i$ | $-0.1020 \pm 1.7380i$ | $-0.1247 \pm 1.4470i$ |
| — | $-0.8847 \pm 1.2464i$ | $-0.7662 \pm 1.1680i$ | $-0.6352 \pm 1.0384i$ |

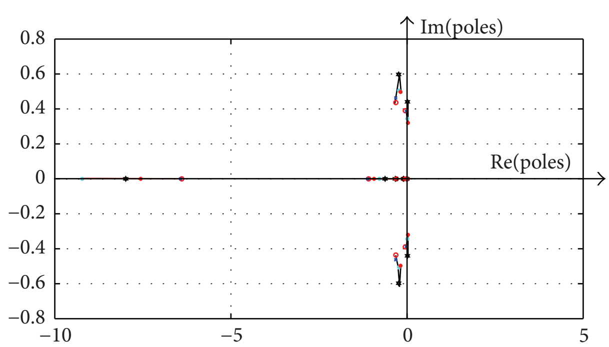


FIGURE 3: System root-locus diagram showing pole locus for constant slung length (15 ft) as load weight is increased.

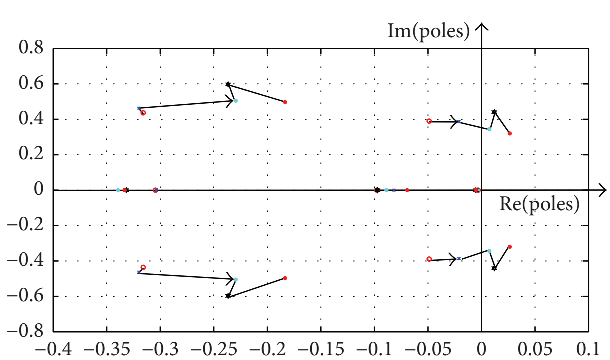


FIGURE 4: Enlarged view of Figure 3 showing poles locus near to Re(poles) = 0 axis.

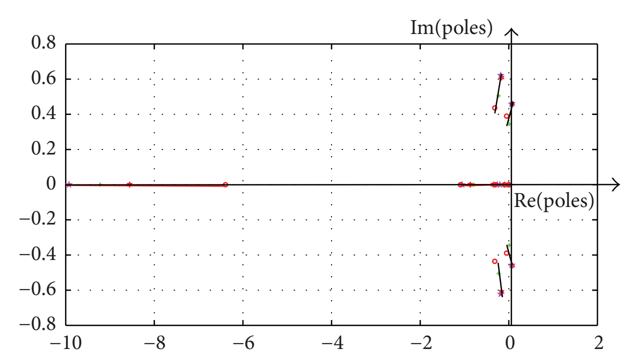


FIGURE 5: System root-locus showing pole locus for constant load weight (1000 lb) as slung length is increased.

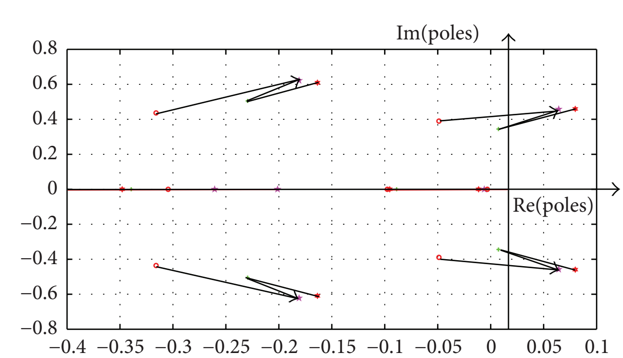


FIGURE 6: Enlarged view of Figure 5 showing poles locus near to Re(poles) = 0 axis.

carries a load weight 500 lb and 1000 lb, then $\alpha_1 = 0.3$ and 0.41 with $\beta_1 = 0.41$ and 0.82, respectively; therefore $\alpha_1 + \beta_1 < 1$; thus the system is stable. But when the load weight is 1500 lb and 2000 lb, then $\alpha_1 = 0.1$ and 0.075 and also $\beta_1 = 1.23$ and 1.64, respectively; therefore $\alpha_1 + \beta_1 > 1$; thus the system is unstable. For the case of the constant load weight (1000 lb) as slung length is increased, then for a 10 ft and 15 ft slung length $\alpha_1 = 0.15$ and $\beta_1 = 0.55$ and 0.82, respectively; therefore $\alpha_1 + \beta_1 < 1$; thus the system is stable. But when the slung length increased to 20 ft then $\alpha_1 = 0.15$ and $\beta_1 = 1.09$; therefore $(\alpha_1 + \beta_1) = 1.24$; that is, $\alpha_1 + \beta_1 > 1$; thus the system is unstable. However, the system can be marginally stable; if the UH-60 helicopter carries a load weight 725 lb by a 20 ft slung length, then $\alpha_1 = 0.2$ and $\beta_1 = 0.8$; therefore $(\alpha_1 + \beta_1) = 1$. For this set of analysis $k_D$ is assumed to be $k_D = 75$ lb/ft. However, $k_D$ can vary depending on the weather condition and an example of $k_D = 50$ lb/ft is shown above for illustrative purpose. This analysis suggests that the maximum value of 20 ft slung length may be used for slung load operation. However, the load weight limit can vary with respect to the capacity of the load carrying hooks, helicopter weight, environmental conditions, and so forth.

The examples presented here show that the simulation results are correlated with the stability analysis. Thus, desired condition for the stability is met and it can locate the load at the specified position or its neighbourhood.

## 5. Conclusions

In this paper stability analysis of a helicopter with an underslung load system is investigated. The investigation identified the conditions for the stabilisation of the system and the positioning of the underslung load at hover condition. Stability analysis and numerical results proved that the desired condition for the stability is met; then it is possible to locate the load at the specified position or its neighbourhood. An illustration example is also given in the paper. The method results in a guaranteed load positioning accuracy which depends on the design parameters and the method can be applicable to any individual helicopter with external load system.

## Nomenclature

$L, M, N$: Overall helicopter rolling, pitching, and yawing moments
$p, q, r$: Helicopter roll, pitch, and yaw rates about body reference axes
$X, Y, Z$: Overall helicopter force components
$\phi, \theta, \psi$: Roll, pitch, and yaw angles
$u, v, w$: Helicopter velocity components at centre of gravity
$\theta_0$: Main rotor collective
$\theta_{1s}$: Longitudinal cyclic commands
$\theta_{1c}$: Lateral cyclic commands
$\theta_{0T}$: Tail rotor collective
$X_0, Y_0, Z_0$: Location of the suspension point with respect to earth referenced $x$, $y$, and $z$ directions
$\dot{X}_0, \dot{Y}_0, \dot{Z}_0$: The helicopter velocity in the $x$, $y$, and $z$ directions
$\ddot{X}_0, \ddot{Y}_0, \ddot{Z}_0$: The helicopter acceleration in the $x$, $y$, and $z$ directions
$\theta_L$: Load suspension angle in the $X$-$Z$ plane with respect to $Z$-axis
$\phi_L$: Load suspension angle in the $Y$-$Z$ plane with respect to $Z$-axis
$M_L$: Mass of the suspended load
$g$: Acceleration due to gravity
$l$: Slung length
$k_D$: Aerodynamic drag force constant ($k_D = (1/2)\rho S C_D$)
$\rho$: Air density
$S$: The load area presented to the airflow
$C_D$: Drag coefficient for the load.

## Competing Interests

The author declares that there are no competing interests regarding the publication of this paper.

## References


[1] K. Thanapalan and F. Zhang, "Modelling and simulation study of a helicopter with an external slung load system," *I-Managers Journal on Instrumentation & Control Engineering*, vol. 1, no. 1, pp. 9–17, 2013.

[2] M. Bisgaard, J. D. Bendtsen, and A. La Cour-Harbo, "Modeling of generic slung load system," *Journal of Guidance, Control, and Dynamics*, vol. 32, no. 2, pp. 573–585, 2009.

[3] *Handling Qualities Requirements for Military Rotorcraft*, ADS-33-D, U.S. Army Aviation and Troop Command, St Louis, Miss, USA, 1996.

[4] K. Thanapalan and T. M. Wong, "Modeing of a helicopter with an under-slung load system," in *Proceedings of the 29th Chinese Control Conference (CCC '10)*, pp. 1451–1456, Beijing, China, July 2010.

[5] B. Feng, "Robust control for lateral and longitudinal channels of small-scale unmanned helicopters," *Journal of Control Science and Engineering*, vol. 2015, Article ID 483096, 8 pages, 2015.

[6] J. J. Gribble, "Linear quadratic Gaussian/loop transfer recovery design for a helicopter in low-speed flight," *Journal of Guidance, Control, and Dynamics*, vol. 16, no. 4, pp. 754–761, 1993.

[7] M. A. Manness, J. J. Gribble, and D. J. M. Smith, "Multivariable methods for helicopter flight control law design," in *Proceedings of the 16th Annual Society European Rotorcraft Forum*, Paper No. III.5.2, Glasgow, UK, September 1990.

[8] W. L. Garrard, E. Low, and S. Prouty, "Design of attitude and rate command systems for helicopters using eigenstructure assignment," *Journal of Guidance, Control, and Dynamics*, vol. 12, no. 6, pp. 783–791, 1989.

[9] Y. B. Shtessel and I. A. Shkolnikov, "Aeronautical and space vehicle control in dynamic sliding manifolds," *International Journal of Control*, vol. 76, no. 9-10, pp. 1000–1017, 2003.

[10] D. F. Thompson, J. S. Pruyn, and A. Shukla, "Feedback design for robust tracking and robust stiffness in flight control actuators using a modified QFT technique," *International Journal of Control*, vol. 72, no. 16, pp. 1480–1497, 1999.

[11] K. Thanapalan, "Modelling of a helicopter system," in *Proceedings of the 1st Virtual Control Conference (VCC '10)*, pp. 45–52, Aalborg University, 2010.

[12] D. P. Goodall and J. Wang, "Stabilization of a class of uncertain nonlinear affine systems subject to control constraints," *International Journal of Robust and Nonlinear Control*, vol. 11, no. 9, pp. 797–818, 2001.

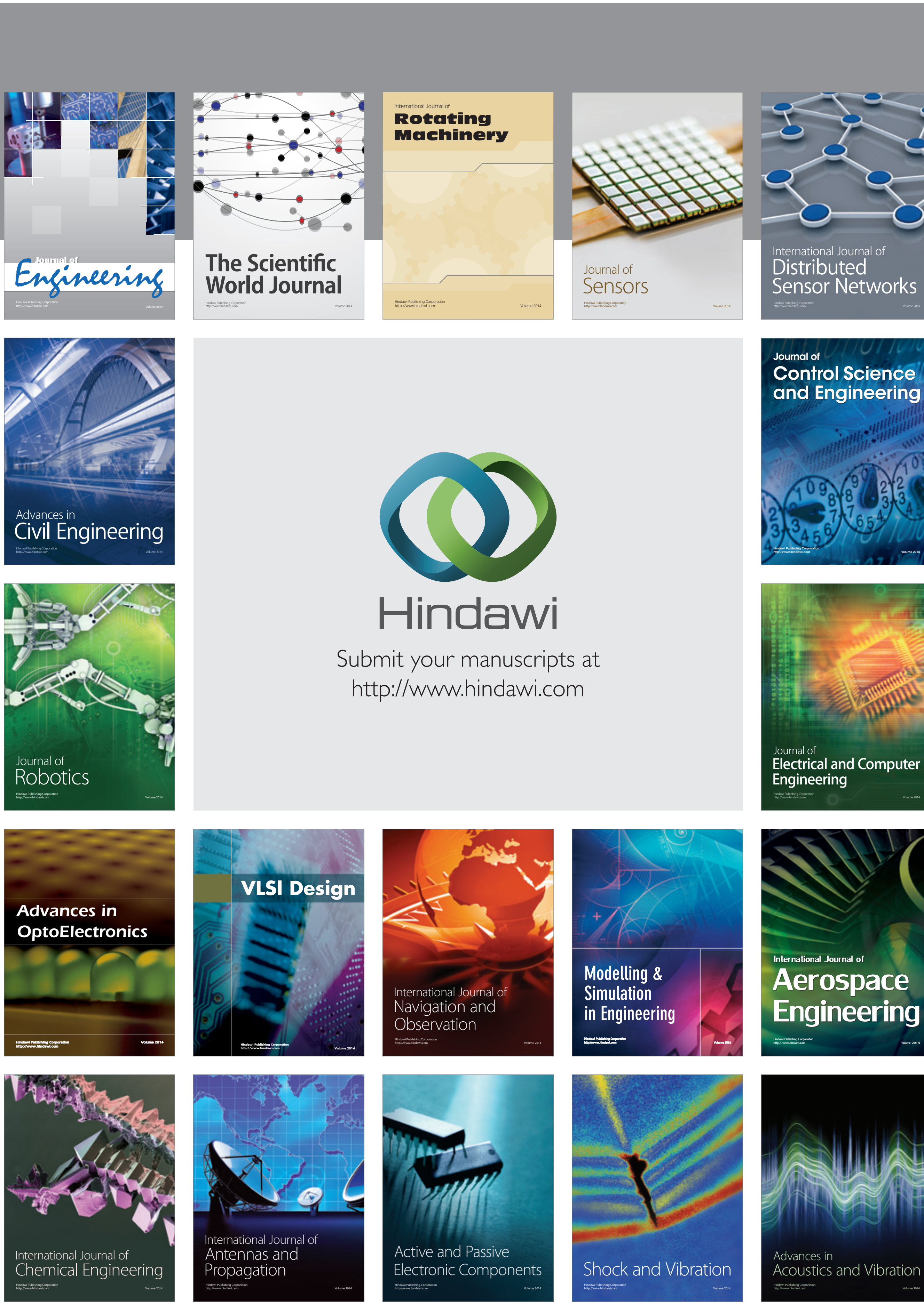
Journal of Engineering
The Scientific World Journal
International Journal of Rotating Machinery
Journal of Sensors
International Journal of Distributed Sensor Networks
Advances in Civil Engineering
Hindawi
Submit your manuscripts at
http://www.hindawi.com
Journal of Control Science and Engineering
Journal of Robotics
Journal of Electrical and Computer Engineering
Advances in OptoElectronics
VLSI Design
International Journal of Navigation and Observation
Modelling & Simulation in Engineering
International Journal of Aerospace Engineering
International Journal of Chemical Engineering
International Journal of Antennas and Propagation
Active and Passive Electronic Components
Shock and Vibration
Advances in Acoustics and Vibration